

REGULATORY INFORMATION DISTRIBUTION SYSTEM (RIDS)

ACCESSION NBR: 8403130144 DOC. DATE: 84/03/02 NOTARIZED: NO DOCKET #  
 FACIL: 50-331 Duane Arnold Energy Center, Iowa Electric Light & Pow 05000331  
 AUTH. NAME: MCGAUGHY, R.W. AUTHOR AFFILIATION: Iowa Electric Light & Power Co.  
 RECIP. NAME: DENTON, H. RECIPIENT AFFILIATION: Office of Nuclear Reactor Regulation, Director

SUBJECT: Forwards response to NRC 840207 request for addl info re plant unique analysis rept for Mdark I torus mods.

DISTRIBUTION CODE: A025S COPIES RECEIVED: LTR 1 ENCL 40 SIZE: 24  
 TITLE: OR Submittal: USI A-7 Mark I Containment

NOTES:

	RECIPIENT		COPIES			RECIPIENT		COPIES	
	ID	CODE/NAME	LTTR	ENCL		ID	CODE/NAME	LTTR	ENCL
	NRR	ORB2 BC 01	4	0					
INTERNAL:	EDO		1	0	ELD/HDS2	13	1	0	
	NRR DIR		1	0	NRR SIEGEL, B		5	5	
	NRR/DE/MEB		4	4	NRR/DE/MTEB		1	1	
	NRR/DL/GRAB	10	1	1	NRR/DSI/CSB	11	1	1	
	REG FILE	04	1	1	RGN3		1	1	
EXTERNAL:	ACRS	12	10	3	LPDR	03	1	1	
	NRC PDR	02	1	1	NSIC	05	1	1	
	NTIS		1	1					

Iowa Electric Light and Power Company

March 2, 1984  
NG-84-0864

Mr. Harold Denton, Director  
Office of Nuclear Reactor Regulation  
U.S. Nuclear Regulatory Commission  
Washington, DC 20555

Subject: Duane Arnold Energy Center  
Docket No: 50-331  
Op. License No: DPR-49  
Mark I Torus Modifications  
Reference: NRC Letter, D. Vassallo to L. Liu, dated  
February 7, 1984

Dear Mr. Denton:

The attachment to this letter provides the information requested by the referenced letter regarding our Plant Unique Analysis Report (PUAR) for our Mark I torus modifications.

If you have any additional questions, please contact us.

Very truly yours,

*R. W. McLaughly*

Richard W. McLaughly  
Manager, Nuclear Division

RWM/SS/ks

Attachment: Response to NRC Request for Additional Information  
Regarding Mark I Containment Plant Unique Analysis Report

cc: S. Swails  
L. Liu  
S. Tuthill  
M. Thadani  
NRC Resident Office  
Commitment Control No: 84-0038

8403130144 840302  
PDR ADOCK 05000331  
PDR

*A025  
1/10*

Attachment  
NG-84-0864  
March 2, 1984

DUANE ARNOLD ENERGY CENTER

DOCKET NO. 50-331

RESPONSE TO NRC REQUEST FOR

ADDITIONAL INFORMATION REGARDING MARK I

CONTAINMENT PLANT UNIQUE ANALYSIS REPORT

Item 1: PUAR Section 1-4.1.4.3, AC Section 2.8

Describe the method used to determine the froth load application direction and duration for the monorail analysis. Indicate which QSTF tests were used and provide sufficient detail to describe how a conservative load specification was achieved.

Response:

The froth (region I) load application direction and duration for the monorail analysis were determined from a detailed analysis of the QSTF plant-specific high speed films (alternate method provided in section 4.3.5.2 of the LDR). Individual movie frames were viewed and analyzed, then drawn to show the pool swell and froth (region I) formation.

From these pictures, the angle swept by the froth was determined to be 0 to 67° from the horizontal. The duration or impingement pulse time was also determined from plant-unique QSTF movies. Specifically, the duration  $\tau$  was obtained from the measured values of froth length  $L_f$ , and froth velocity  $V_f$  ( $\tau = L_f/V_f$ ).

DAEC has a partial vent header deflector in the vent bay and a full deflector in the non-vent bay. For this reason, two sets of QSTF tests were analyzed (IOWA-unique): Test 5 which was the only test performed with no deflector at zero  $\Delta P$ , and tests 6, 7 & 8 which were performed with the deflector at zero  $\Delta P$ .

The froth (region I) load on the monorail was determined using the alternate method as mentioned previously. The froth impingement pressure is given by

$$(1) \quad P_f = \frac{\rho_f V_f^2}{g_c 144}$$

where

$V_f$ : is the froth source velocity (ft/sec)  
 $\rho_f$ : is the froth density ( $lb_m/ft^3$ )

The froth velocity was measured from the IOWA-unique tests and the froth density is given by

$$(2) \quad \rho_f = \frac{M_f/L}{W_f V_f \tau} \quad (\text{LDR Section 4.3.5.2})$$

$$\rho_f = \frac{M_f/L}{\frac{W_f V_f L_f}{V_f}} = \frac{M_f/L}{W_f L_f}$$

where

$W_f$ : width of froth (ft)  
 $L_f$ : length of froth (ft) (thickness)  
 $L$ : azimuthal length of froth (ft) around torus  
 $M_f$ : mass of froth ( $lb_m$ )

The width ( $W_f$ ) and the length or thickness ( $L_f$ ) were measured from the IOWA-unique tests;  $L$  is the azimuthal length, and the froth mass is given by

$$(3) \quad M_f = \frac{M_h/2}{\left(\frac{V_f}{V_i}\right)^2 - \frac{V_f}{V_i} \sin \theta} \quad (\text{LDR Section 4.3.5.2})$$

where

$M_h$ : is the hydrodynamic mass of the vent header (test 5) or the vent header deflector (tests 6, 7 & 8) ( $lb_m$ )

$\theta$ : is the mean jet angle

The mean jet angle was measured from IOWA-unique tests while the hydrodynamic mass  $M_h$  was obtained from

$$(4) \quad I = \frac{M_h V_i}{g_c}$$

where  $I$  is the impulse on the vent header and  $V_i$  is the vent header impact velocity, both of which were measured during test 5 (IOWA-unique); or  $I$  is the impulse on the vent header deflector and  $V_i$  is the vent header deflector velocity measured during tests 6, 7 & 8 (IOWA unique). When calculating the hydrodynamic mass ( $M_h$ ) for tests 6, 7 & 8, only  $M_h$  for the vent header deflector is accounted for because there was no measured load on the vent header.

To ensure a conservative load definition, the following steps were taken:

- o The froth velocity used in calculating the froth mass (equation 3) was the lowest one from tests 6, 7 & 8, which maximizes the froth mass.
- o The froth velocity used in calculating the froth impingement pressure (equation 1) was the highest one from tests 6, 7 & 8, which maximizes the froth impingement pressure.
- o The froth velocity was not decelerated due to gravity, thereby increasing the froth impingement pressure.
- o The froth width ( $W_f$ ) and thickness ( $L_f$ ) used in calculating the froth density (equation 2) were measured values near the vent header deflector. These parameters have bigger values at the monorail which would result in lower densities, and larger froth loads.

The froth (region II) load on the monorail was defined following the LDR methodology.

Item 2: PUAR Section 1-4.1.6

The submergence listed in Table 1-2.2-1 for high water level (3.39 ft.) is not consistent with the submergence in Table 1-4.1-2 (3.333 ft.). Clarify the issue by specifying the current maximum value of downcomer submergence.

Response:

The downcomer submergence listed in PUAR Table 1-2.2-1 for high water level (3.39 ft) corresponds to maximum  $\Delta P$ . The submergence in PUAR Table 1-4.1-2 (3.333 ft) corresponds to zero  $\Delta P$ . All the analysis for DAEC was performed based on zero  $\Delta P$ , as it would result in conservative loads. Therefore, Table 1-2.2-1 in the PUAR should read 3.333 ft. for the downcomer submergence.

Item 3: PUAR section 1-5.2, AC section 2.13.8

Provide the following information pertaining to the Suppression Pool Temperature Monitoring System Design (SPTMS):

- a) A sketch which shows the circumferential locations of the sensors with respect to the T-quencher locations in a plan view such as Figure 1-2.1-5.

Response: The attached Bechtel drawing (Figure 3-1) shows the circumferential location of both trains of SPTMS Temperature Sensors in relation to the six T-quenchers.

Item 3: b) In addition, indicate on this sketch, the direction of the RHR nozzle discharges and the T-quencher arms which have end cap holes.

Response: Superimposed on the attached Bechtel drawing is the location of the two RHR discharge nozzles and a note identifying the hole end of the T-quenchers.

Item 3: c) Provide more details on the correlation between the local and bulk temperatures.

Response: A detailed thermo-hydrodynamic analysis of the Duane Arnold Plant specific Configuration was performed by General Electric using their T-pool model which has been correlated with the Monticello test data.

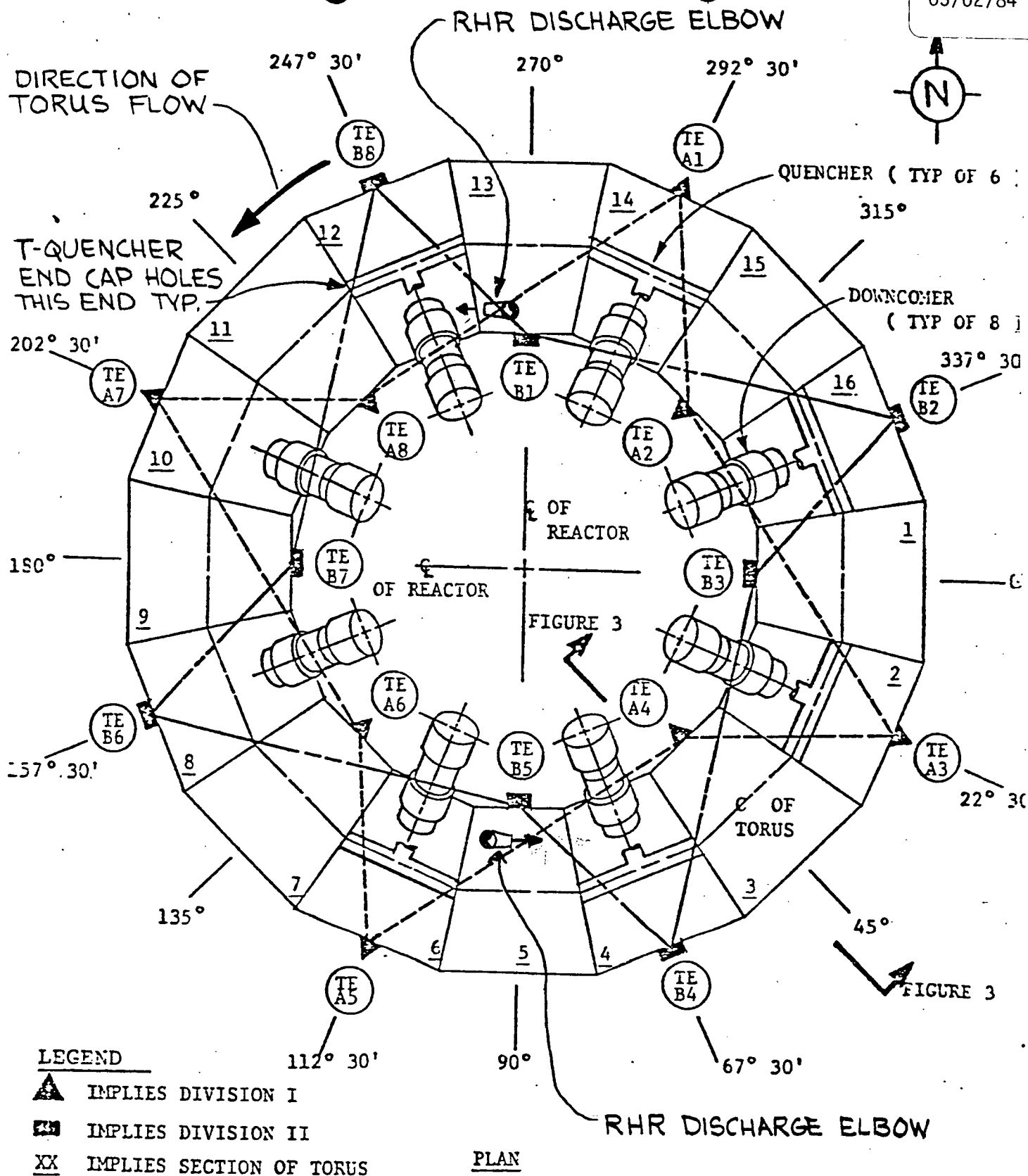


FIGURE 3-1

Item 4(a): The NUREG-0661 acceptance criteria in Section 2.13.9 describes a procedure whereby SRV in-plant tests may be used to calibrate the coupled load-structure analytical model to the measured pressure wave form and structural response. However, the statement on page 1-4.77 of the PUAR states that the "plant unique SRV testing at DAEC has been performed to confirm that the computed loadings and predicted structural responses for SRV discharges are conservative". Clarify the issue by providing a detailed description of what was done to define the SRV discharge loads. Was the LDR QBUBS methodology used?

Response:

The SRV discharge loads were generated using the General Electric QBUBS program following the LDR methodology. The loads were generated for various load cases, i.e., for the normal operating and accident conditions and for the first and subsequent actuations to bound the amplitude and frequency of the SRV load. Frequency bands of  $\pm 25$  percent on the first actuation and  $\pm 40\%$  on the subsequent actuation were applied as specified in the LDR Section 5.2.2.3. Also as per NUREG-0661 acceptance criteria, pressure amplitude predicted for the SRV first actuation was used in conjunction with the bubble frequency range for subsequent actuation to maximize the response due to SRV loads. Torus shell loads due to multiple SRV actuation were calculated by summing absolutely the peak values of shell pressure due to a single valve actuation with the appropriate pressure attenuation model.

The paragraph on PUAR page 1-4.77 summarizes that the structural response measurements of the DAEC in-plant tests were used to calibrate a coupled load-structure analytical model for SRV load evaluation. The comparison between the values predicted from the analytical model and the measured values from the in-plant tests are shown in the PUAR Table 1-4.2-5. The comparison shows that the analytical model used to evaluate the SRV loads predicts conservative responses.

Item 4(b): It is asserted on page 1-4.92 that "to account for the variation in the hydrodynamic characteristics of the SRV discharge line configuration, loads are generated for the shortest and longest SRV line and the higher of the two loads is used in the analysis". Describe why this procedure will conservatively bound all possible loads. Does this explain why Figure 2-2.2-14 uses the shortest SRVDL for the SRV discharge torus shell load case A1.2/C3.2 for multiple actuations?

Response:

The statement on page 1-4.92 quoted above refers to the loads on the torus shell due to SRV actuation. In order to ensure a bounding load definition on the torus shell due to SRV discharge, every SRVDL would have to be analyzed. However, only the shortest and the longest SRVDL need to be analyzed because they would provide the maximum bound for the pressure amplitude and frequency band. The longest line has the largest air volume and therefore will provide the highest bubble pressure and torus shell pressure as shown by the 1/4 scale test for T-quenchers. Similarly, shortest line with the smallest air volume produces the upper bound on the load frequency and longest line will produce the lower bound on frequency. The shortest and longest line analyzed for all the cases summarized in response to Item 4(a) will therefore conservatively bound all possible loads.

The following table summarizes the air volumes for the shortest and longest SRVDLs for DAEC, as a function of load case. These values were used in the generation of SRV discharge loads on the torus shell and sub-merged structures.

SRVDL	Air Volume (ft <sup>3</sup> )		
	Case		
	Al.1	Al.2/C3.2	C3.1
GBC-9	52.909	54.568	52.241
GBC-10	40.492	42.152	39.825

Case Al.2/C3.2 in the PUAR Figure 2-2.2-14 is the case where pressure amplitude from the first actuation is used in conjunction with the bubble frequency range for subsequent actuation. However, the term shortest SRVDL is incorrect in this figure. The pressure values shown in this figure are again from the longest SRVDL, as pressures from longest SRVDL are larger than those from the shortest SRVDL.

Item 4(c): Describe in detail how the calibration factors (page 1-4.103) were developed from the in-plant tests conducted at DAEC for use in the determination of the drag loads on SRV lines, elbow support beams, T-quenchers and their supports, and vent header support columns. Include as part of your response, the various test data, instrumentation layout with respect to quencher location, etc. used to derive the factors. Justify the use of these factors for the design SRV discharge event cases.

Response:

Calibration factors for use in the determination of the drag loads on SRV lines, elbow support beams, T-quenchers and their supports, and vent header support columns were developed from the in-plant tests conducted at DAEC. The factors are based on the ratio of the analytical results at test conditions divided by the actual measured test results. The loading applied to the analytical model was developed with the same initial conditions as the actual test. The analytical loading included SRV discharge thrust, air-bubble drag, uneven clearing thrust, and internal pressure loads. The effect of torus motions was conservatively not included in the analytical results used for the generation of calibration factors.

For SRV line, elbow support beam, and the vent header support columns, strain from the analysis at test condition was compared to the maximum strain from all the SRV in-plant tests at the location of strain gages in a particular structure. The resulting factor for each structure was applied to the design stress results for that structure. Thus, calibration factors

were developed at test conditions and then applied at design basis conditions, as recommended by NUREG-0661 acceptance criteria section 2.13.9.

For the T-quencher and its support beam, measured data from pressure transducers on the quencher were utilized in determining the SRV discharge drag loads on these structures. The analytical bubble pressure was divided by the test bubble pressure for the same initial conditions. Calibrated bubble pressure was used in calculating the SRV discharge air-bubble drag loads on the T-quencher and its support beam.

Location and orientation of strain-gages used in the derivation of calibration factors for SRV line (strain gages 31-34), elbow support beam (strain gages 35-38 and 147-148), and vent header support columns (strain gages 143-146) are shown in the attached Figure 4-1. The pressure transducers  $P_1$  through  $P_4$  on the quencher are shown in the attached Figure 4-2. Typical strain time histories measured in the in-plant test are shown in Figures 4-3 and 4-4.

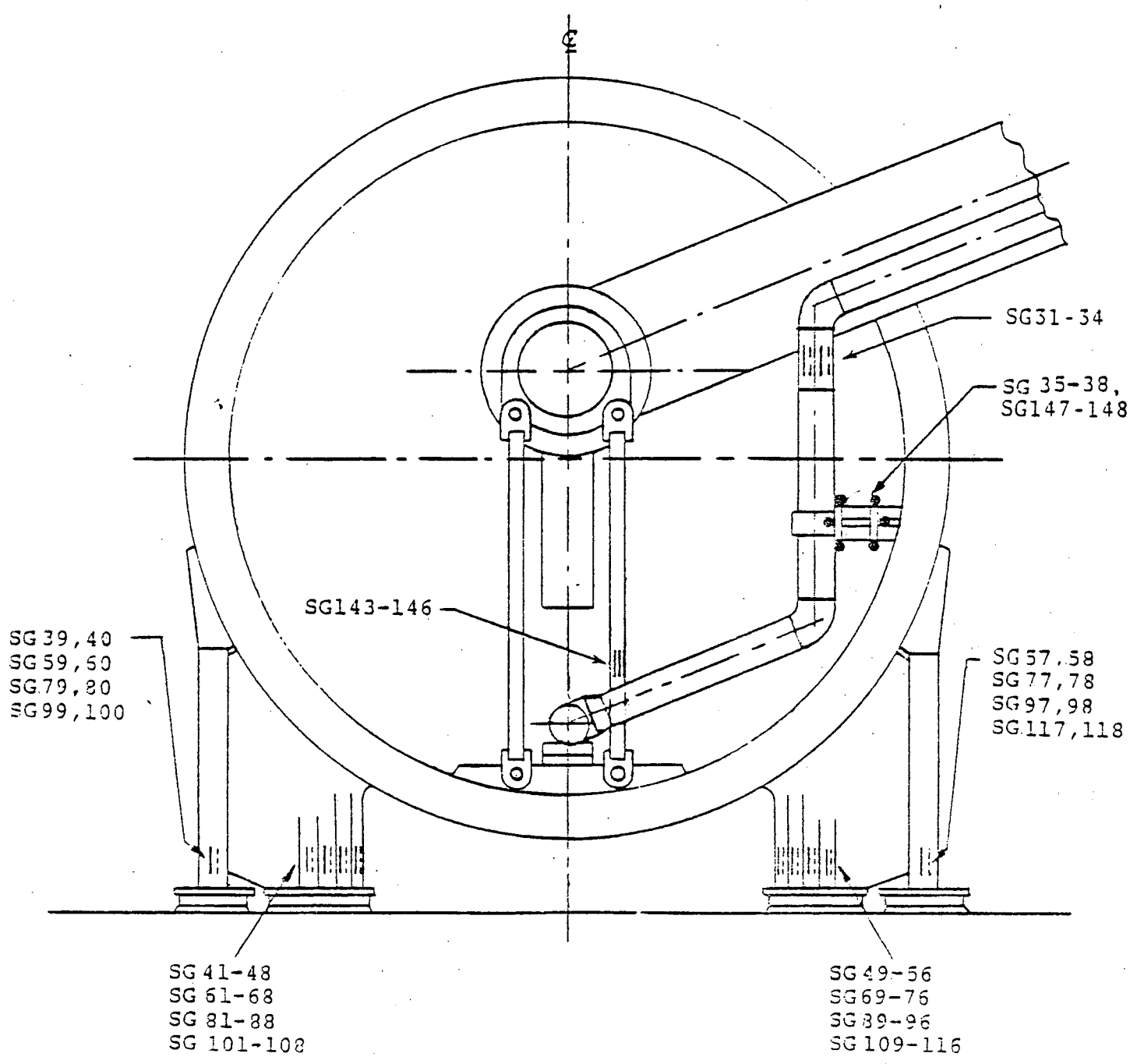


Figure 4-1  
STRAIN GAGE LOCATIONS ON THE SRV PIPING, ELBOW  
SUPPORT BEAM, AND VENT HEADER SUPPORT  
COLUMNS IN THE TEST BAY

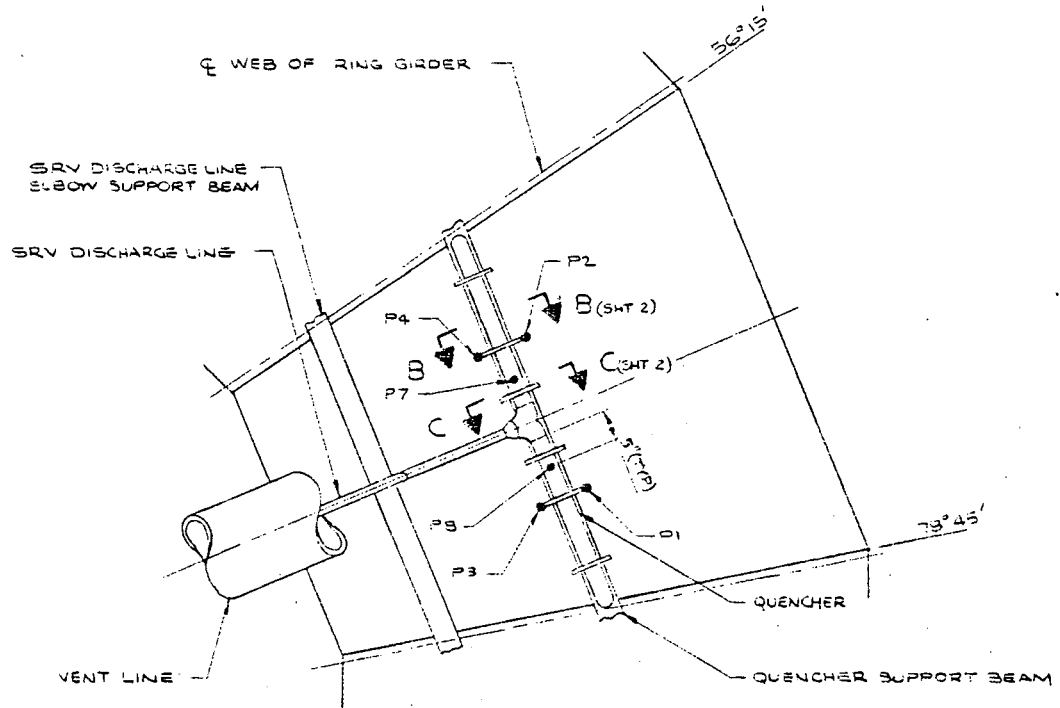


Figure 4-2

PRESSURE TRANSDUCERS ON QUENCHER

16

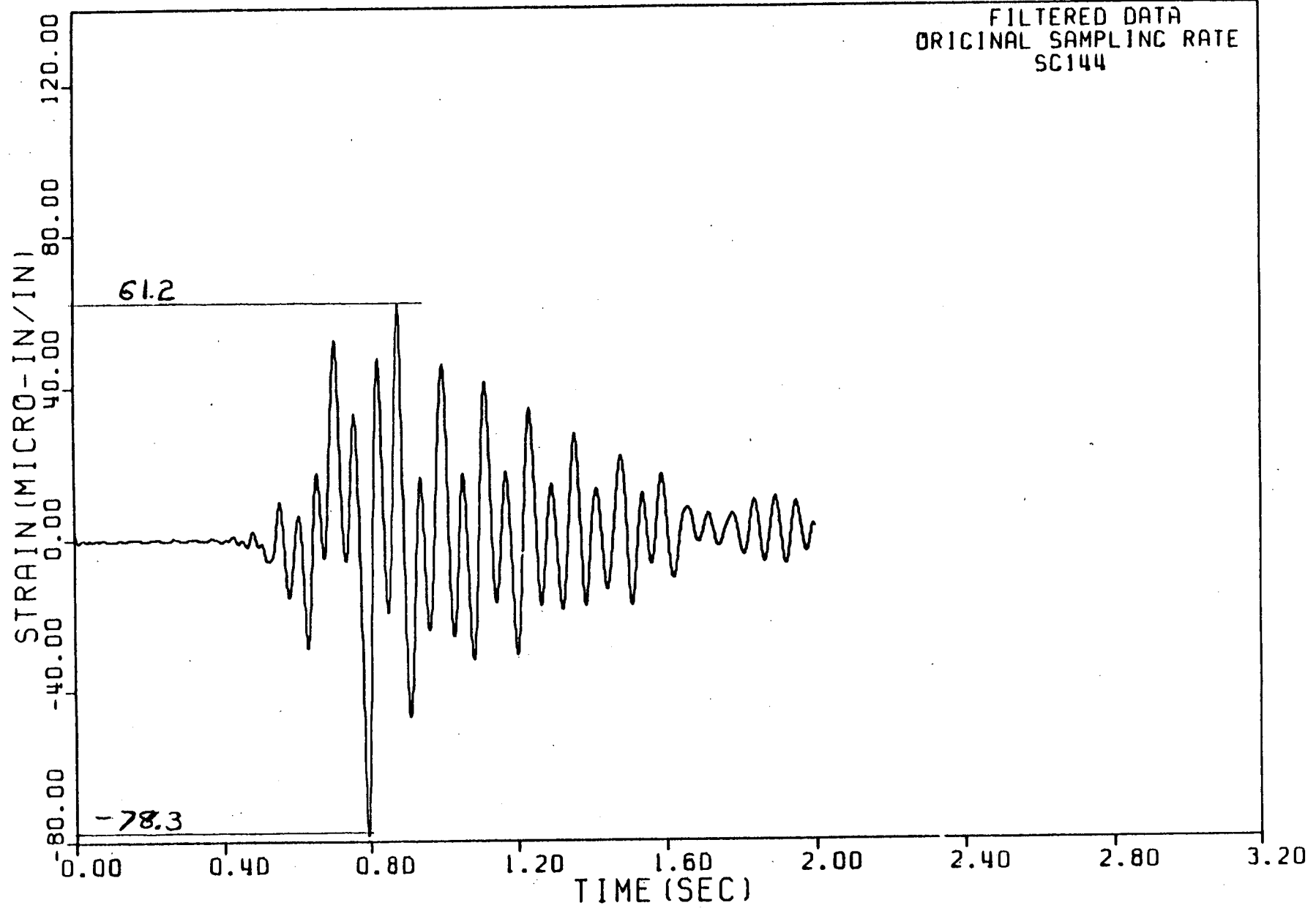


Figure 4-3

# DUANE ARNOLD IN-PLANT SRV TEST MT5

Attachment  
NG-84-0864  
03/02/84

FILTERED DATA  
ORIGINAL SAMPLING RATE  
SC146

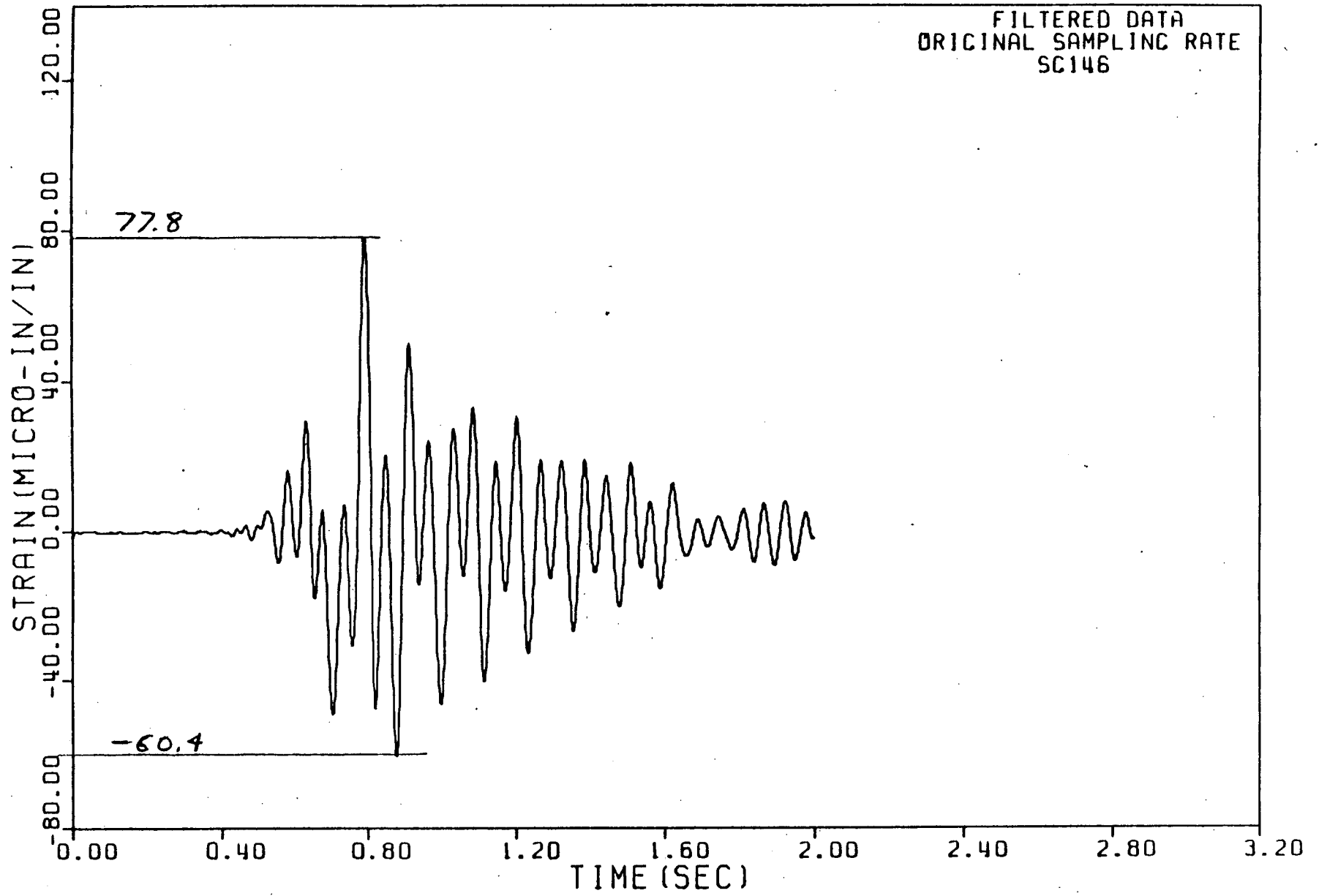


Figure 4-4

DUANE ARNOLD IN-PLANT SRV TEST MT5

Attachment  
NG-84-0864  
03/02/84

Item 5:

The LDR submerged structure load definition requires the specification of a source strength at the downcomer which was derived from the FSTF test series. It is not clear from the reading of the DAEC PUAR exactly what source strengths were used for both the CO and chugging load evaluations. For instance, on page 2-2.31 it is stated that the DBA CO submerged structure loads were developed for the case with the maximum source strength at the nearest downcomer. However, on page 3-2.36, it is said that the same loads were developed for the case with the average source strength at all downcomers and for the case with twice the average source strength at the nearest downcomer. In order to resolve the confusion indicate which source strengths were used in both the CO and chugging evaluations.

Response:

As per the NUREG-0661 acceptance criteria sections 2-14.5 and 2-14.6, submerged structure loads due to condensation oscillation and pre-chug were computed on the basis of both the average source strength at all downcomers and for the maximum source strength applied at the nearest downcomer. Similarly, post-chug submerged structure loads were computed on the basis of the two nearest downcomers chugging at the maximum source strengths, with phasing between the downcomers that maximizes the local acceleration. The loads were first generated with a unit source strength and then multiplied by the average or the maximum source function at various frequencies. The average source strength as a function of frequency used for the DAEC condensation oscillation submerged structure loads are listed in PUAR Table 1-4.1-9 and for pre and post-chug

submerged structure loads in PUAR Table 1-4.1-12. These source strengths are derived from the FSTF test series. The maximum source strength at a given frequency is obtained by multiplying the average source strength at that frequency by a factor of two.

The statement in DAEC PUAR page 2-2.31, which states that the condensation oscillation submerged structure loads were developed using the maximum source strength is incorrect. The condensation oscillation loads were developed based upon the average source strength. Similarly statement on PUAR page 3-2.42, which states post-chug submerged structure loads were generated using average source strength, should read as generated using the maximum source strength.

Item 6: A number of LDR load definitions such as CO and chugging torus loads, downcomer lateral loads, submerged structure loads, etc. have been derived from the FSTF facility which had a prototypical Mark I downcomer configuration. Comment on why it is appropriate to apply these load definitions in the DAEC plant-unique analysis considering the fact that DAEC has a single downcomer geometry. Include a discussion of the applicability of the source strengths obtained from FSTF in the DAEC evaluation. How does the DAEC steam mass flow per downcomer compare with the FSTF value?

Response:

Condensation oscillation and chugging loads were derived from the results of tests conducted in the FSTF which was a full scale, 22.5° sector of a typical Mark I torus connected to simulated drywell and pressure vessel volumes. Principal design parameters for the FSTF, such as vent-area to pool-area ratio and distance of the downcomer exit to the torus shell were selected to produce conservative data from which the loads for all Mark I plants could be derived.

To calculate condensation oscillation torus shell loads for plant unique application, LDR defines a multiplication factor to account for the effect of different pool to vent area ratio in a plant as compared to FSTF. This factor as applied to DAEC is given in PUAR Figure 1-4.1-9. As is evident from this figure, FSTF pool to vent area ratio was chosen such that it would result in most conservative loads.

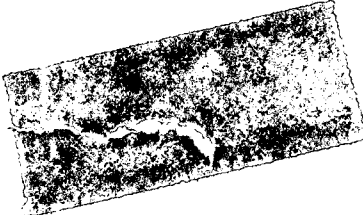
For condensation oscillation downcomer lateral loads, LDR Section 4.4.3 states that there are no differential pressure downcomer lateral loads for Duane Arnold as it has only a single vertical downcomer.

For chugging loads, the chugging behavior observed in the prototypical FSTF tests would be similar in nature to the chugging behavior in DAEC, since the chugging source strength is primarily controlled by thermodynamic and geometric conditions at the vent exit. These conditions such as the downcomer diameter and the downcomer submergence for DAEC are similar to other Mark I plants and the FSTF.

Downcomer lateral load due to chugging is defined in the LDR as a Resultant Static Equivalent Load (RSEL) which, when applied statically to the end of the downcomer, will produce the measured bending response near the downcomer/vent header junction. The maximum design load for DAEC was obtained by scaling the maximum RSEL for the FSTF configuration. The scaling factor was derived on the basis of a comparison of the dynamic characteristics of DAEC downcomers and the FSTF as shown in PUAR Table 3-2.2-10. Thus, chugging lateral load accounts for the plant unique DAEC characteristics.

When generating submerged structure loads due to condensation oscillation and chugging, plant unique DAEC geometries with single downcomers were used. The source strengths used in these calculations are as given in PUAR Tables 1-4.1-9 and 1-4.1-12. These source strengths were derived from the wall pressure measurements in FSTF. As mentioned earlier, the

parameters selected in FSTF are such that the wall pressure measurements are conservative in FSTF as compared to all the Mark I plants. Also, for plants with downcomers in a pair, spacing between the downcomer exit and the wall in general is smaller than the DAEC plant with a single downcomer in the middle, resulting in smaller loads for DAEC in case of a LOCA.



The DBA pipe break area for the FSTF was chosen as  $0.442 \text{ ft}^2$  (Table A-1, FSTF report NEDO-24539). Therefore pipe break area per downcomer in FSTF was  $0.055 \text{ ft}^2$  (obtained by dividing the total break area by 8 downcomers). The largest break area for DAEC (recirculation line break area) is  $2.515 \text{ ft}^2$  (LDR Table 4.1.1-4). Therefore for DAEC the break area per downcomer is  $0.052 \text{ ft}^2$  (obtained by dividing the total break area by 48 downcomers). Thus, break area per downcomer which is a measure of the steam mass flow per downcomer is similar for the FSTF and DAEC.